New Fractional Frequency Reuse Patterns for Multi-Cell Systems in Time-Varying Channels

Pochun Yen, Qi Zhan, Hlaing Minn, *Senior Member, IEEE*

***Abstract*—Fractional frequency reuse (FFR) and exploitation of the channel state information at the transmitter (CSIT) are effective approaches to improve the spectrum efficiency of the outer coverage region. When channels vary within a physical transmission frame, the above improvement is substantially suppressed. To remedy this, this paper develops new FFR patterns for multi-cell OFDMA systems with frequency or time division duplexing (FDD/TDD) in time-varying channels. Simulation results show notable performance gains of the proposed schemes over the existing ones.**

***Index Terms*—Fractional frequency reuse, Soft frequency reuse, Time-varying CSIT accuracy, Spectrum efficiency.**

I. Introduction

The demand for high spectrum efficiency leads to the use of a more aggressive frequency reuse pattern which however degrades the performance of the outer coverage region due to the increased level of inter-cell interference (ICI) [1]. Fractional frequency reuse (FFR) [2]–[4] has emerged as an effective method to reduce ICI level. For capacity enhancement, recent systems exploit channel state information at the transmitter (CSIT). However, when channels vary within a physical transmission frame, the CSIT exploitation gain is substantially suppressed [5], [6]. This issue is addressed for a single-cell system in [7], [8] and for multiple frequency division duplexing (FDD) based systems in [9]. However, such issue has not been studied in the context of FFR, and this problem is important since current and future wireless systems aim to support high mobility with high spectrum efficiency [10] which is a major challenge for outer coverage zones.

This paper addresses how to enhance the spectrum efficiency of outer zones in time-varying channels (a bottle-neck issue of cellular systems). Following the concept of enhancing CSIT exploitation gain in [9], we propose new FFR patterns for multi-cell orthogonal frequency-division multiple access (OFDMA) systems in FDD and time division duplexing (TDD) setups. The new patterns use more (less) spectrum resources at the beginning (later part) of each physical frame where its CSIT accuracy is high (low) to enhance the performance.

II. System Model and CSIT-based Performance Metric

We consider a multi-cell OFDMA system with $N_{\rm DFT}$ subcarriers (either downlink (DL) or uplink (UL)) with either FDD or TDD. Each transmission frame consists of $N_{\rm sym}$ OFDMA symbols (with symbol duration T_s). We consider the two most common types of FFR [10]: strict FFR in a sectorized system and soft frequency reuse (SFR) as the reference schemes. Their cell structure, coverage zoning, and frequency assignment are shown in Fig. 1. There are 3 outer coverage zones $\{Z_1, Z_2, Z_3\}$ and 3 inner zones $\{Z_4, Z_5, Z_6\}$. The overall spectrum is divided into disjoint segments $\{f_i\}$ and they are assigned to those zones such that the inner zones have a lower frequency reuse factor for spectrum efficiency improvement while the outer zones apply a larger frequency reuse factor to reduce the ICI level.

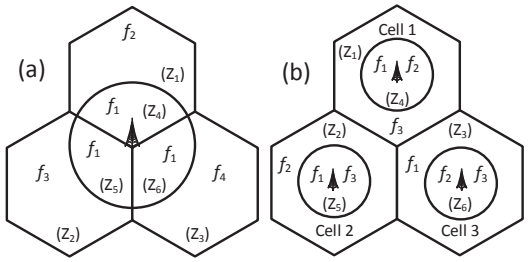

Fig. 1. Zone structure $\{Z_i\}$ and assignment of frequency chunks $\{f_i\}$ in (a) Strict FFR and (b) SFR.

Each base stations (BS) has CSIs of all of its users at the beginning of each physical transmission frame. The CSI acquisition rate is equal to the frame rate. The CSIT accuracy is affected by errors in channel estimation, quantization and feedback, and it is degrading within a frame due to time-varying channels. We follow the same CSIT inaccuracy model in [9]. The channel of a user has L sample-spaced uncorrelated taps with Rayleigh fading envelope and the normalized temporal correlation function $R_t(\tau)$ for each tap gain. Let $H_i[k,n]$ denote the lowpass-equivalent channel gain of a user on the subcarrier k of OFDMA symbol n in zone i with $n \in \{0, 1, \cdots, N_{\rm sym}-1\}$, where channel gains of different users are assumed independent and identically distributed and the user index is omitted for simplicity. Then, the temporal correlation function of $H_i[k,n]$, $\rho_i[m] \triangleq E[H_i[k,n]H_i^*[k,n+m]]$, reads as [9]

$$\rho_i[m] = \frac{1}{N_{\rm DFT}} R_t(mT_s) + \frac{2}{N_{\rm DFT}^2} \times \sum_{c=1}^{N_{\rm DFT}-1} (N_{\rm DFT}-c) R_t\left(\left(m+\frac{c}{N_{\rm DFT}}\right)T_s\right). \quad (1)$$

P. Yen, Q. Zhan and H. Minn (contact author) are with the Department of Electrical and Computer Engineering, University of Texas at Dallas, Richardson, TX, 75080, USA. (e-mail:pxy062000, qi.zhan, hlaing.minn@utdallas.edu).

Thus, $H_i[k,n]$ and $H_i[k,n+m]$ are related as

$$H_i[k,n+m] = \rho[m]H_i[k,n] + \sqrt{1-|\rho_i[m]|^2}\; w_i[k,n+m], \quad (2)$$

where $w_i[k,n+m] \sim \mathcal{CN}(0,1)$ is independent of $H_i[k,n]$.

Suppose CSIT is obtained at μ OFDMA symbols earlier than the beginning of the current physical transmission frame and is denoted by $\hat{H}_i[k,-\mu]$. The error $e_i[k] \triangleq \hat{H}_i[k,-\mu] - H_i[k,-\mu]$ represents imperfection in estimation, quantization, and feedback. There exist several approaches for CSI estimation, quantization, and feedback mechanism, and treating them individually is out of the scope of this paper. As a general treatment, we incorporate their effects in the CSI error term $e_i[k]$ and will assess the performance at various error levels. We assume $e_i[k] \sim \mathcal{CN}(0,\sigma_e^2)$ (i.e., worst case distribution for the corresponding interference) and $\hat{H}_i[k,-\mu] \sim \mathcal{CN}(0,\sigma^2_{\hat{H}})$ since $H_i[k,-\mu] \sim \mathcal{CN}(0,1)$. Then from (2), the CSIT accuracy model becomes

$$H_i[k,n] = \rho_i[n+\mu]\hat{H}_i[k,-\mu] + v_i[k,n], \quad (3)$$

where $v_i[k,n] \triangleq \sqrt{1-|\rho_i[n+\mu]|^2}\; w_i[k,n] - \rho_i[n+\mu]e_i[k]$ represents the combined effect of time-varying channel and CSIT error, and $v_i[k,n] \sim \mathcal{CN}(0,\sigma^2_{v_i}[n])$ with $\sigma^2_{v_i}[n] = \sigma_e^2|\rho_i[n+\mu]|^2 + 1 - |\rho_i[n+\mu]|^2$.

Now, with the temporal correlation in (2) and the CSIT inaccuracy in (3), we introduce the two effective Signal-to-noise ratios (SNRs) given in [9]. Denote ζ_i to be the path loss and σ^2_{N}, σ^2_{I} and σ^2_{ICI} as the powers of noise, inter-carrier interference, and ICI, respectively. Then, the first one reads as

$$\gamma^{(i)}_{\hat{H}}[k,n] = \frac{P^{(i)}_{\mathrm{tx}}\zeta_i\; |\rho_i[n+\mu]\hat{H}_i[k,-\mu]|^2}{\mathcal{I}}, \quad (4)$$

where $\mathcal{I} \triangleq \sigma^2_{\mathrm{N}} + \sigma^2_{\mathrm{I}} + \sigma^2_{\mathrm{ICI}} + P^{(i)}_{\mathrm{tx}}\zeta_i(1-|\rho_i[n+\mu]|^2(1-\sigma_e^2))$ and $P^{(i)}_{\mathrm{tx}}$ is the transmit power. When the transmitter has $\hat{H}_i[k,-\mu]$ only but not $\rho_i[n+\mu]$, the second effective SNR [9] is given as

$$\gamma^{(i)}_{\hat{H}}[k,n] = \frac{P^{(i)}_{\mathrm{tx}}\zeta_i|\hat{H}_i[k,-\mu]|^2}{\mathcal{I} + P^{(i)}_{\mathrm{tx}}\zeta_i|\hat{H}_i[k,-\mu]|^2|1-\rho_i[n+\mu]|^2}. \quad (5)$$

For system performance metric, the CSIT-based data rate $C_i[k,n]$ (conditioned on CSIT $\hat{H}_i[k,-\mu]$) on subcarrier k of OFDMA symbol n in zone Z_i is computed as

$$C_i[k,n] = \log_2\left(1+\gamma^{(i)}_{\hat{H}}[k,n]\right), \quad (6)$$

where $\gamma^{(i)}_{\hat{H}}[k,n]$ is given by either (4) or (5). Let the indexes $\{(k,n)\}$ of the subcarriers assigned to Z_i over the time-frequency grid of a transmission frame be denoted by the resource map $\mathbb{M}_i$ whose size is $|\mathbb{M}_i| = M_i$. Then the CSIT-based data rate (bits/second/Hz) of Z_i is given as

$$C_i = \frac{1}{M_i}\sum_{(k,n)\in\mathbb{M}_i} C_i[k,n]. \quad (7)$$

III. Proposed FFR Patterns

Here, we develop new FFR patterns for improving spectrum efficiency of CSIT-exploiting multi-cell systems in time-varying channels. The coverage zone structures remain the same as in the reference FFR schemes (see Fig. 1). However, the proposed schemes modify the frequency assignment such that for each of the target zones the amount of resources with high CSIT accuracy is larger than the reference schemes while the total resource amount per frame remains the same. For FDD, the proposed schemes intentionally introduce disparities in CSIT accuracy level among different zones through frame offsets. With different frame offsets among zones, every zone can take advantage of using more spectrum resources when its CSIT accuracy is still high at the beginning part of each frame, and less spectrum resources when its CSIT accuracy is degraded at the later part of each frame. Thus, every zone gains spectrum efficiency improvement. However, for TDD, introducing frame offsets as in FDD is not affordable due to heavy interferences between UL and DL. Spectrum efficiency improvement of outer zones is more challenging due to ICI, larger path losses, and peak power constraint. Thus, for TDD, the proposed schemes assign to outer zones more spectrum resources when their CSIT accuracy is high (i.e., at the beginning part of each frame) and less resources when their CSIT accuracy is degraded (i.e., at the later part of each frame). The inner zones get the opposite assignment but their potential spectrum efficiency loss can be easily overcome by increasing their transmit power (as they have lower pathloss) while satisfying power constraint.

The proposed FFR patterns are not channel-adaptive but they are designed to yield better CSIT-exploitation gains. In the following, we present our FFR schemes for four different cases where the resource amount per frame for each zone is kept the same as in the reference schemes.

Case 1 (New Strict FFR in FDD Systems): The top part of Table I presents the proposed scheme. Each spectrum chunk f_i of the reference strict FFR is divided into two chunks f_{ia} and f_{ib} where the resource amount of f_{ib} denoted by $|f_{ib}|$ is kept the same for all i. The frame offset τ_i OFDMA symbols of zone Z_i is set as $\tau_1 = 0$, $\tau_2 = \frac{N_{\mathrm{sym}}}{4}$, $\tau_3 = \frac{2N_{\mathrm{sym}}}{4}$, $\tau_4 = \tau_5 = \tau_6 = \frac{3N_{\mathrm{sym}}}{4}$. Each frame is divided into 4 time periods (TPs) with $\frac{N_{\mathrm{sym}}}{4}$ (= integer) OFDMA symbols each. In all the tables, the beginning of the TP denoted with "*" indicates the beginning of the physical frame for that zone, and the resource map repeats for successive frames. Each zone has a larger spectrum amount at the beginning of its frame where CSIT accuracy is high.

Case 2 (New Strict FFR in TDD Systems): The proposed scheme is shown at the bottom part of Table I. As mentioned before, there are no frame offsets. The proposed scheme divides f_1 into 4 chunks $\{f_{1a}, f_{1b}, f_{1c}, f_{1d}\}$ and f_i for $i = 2,3,4$ into two chunks $\{f_{ia}, f_{ib}\}$ with the resource amounts $|f_{1b}| = |f_{2b}|$, $|f_{1c}| = |f_{3b}|$, and $|f_{1d}| = |f_{4b}|$. Each frame (UL or DL) is divided into two TPs of $\frac{N_{\mathrm{sym}}}{2}$ (=integer) symbols each, and the outer zones (Z_1, Z_2, Z_3) get more spectrum resources during their respective first TP where their CSITs are more fresh.

TABLE I
BANDS ASSIGNMENT FOR NEW STRICT FFR

		Z_4, Z_5 and Z_6	Z_1
FDD	TP1	f_{1a}	* f_2 f_{1b} f_{3b} f_{4b}
	TP2	f_{1a}	f_{2a}
	TP3	f_{1a}	f_{2a}
	TP4	* f_1 f_{2b} f_{3b} f_{4b}	f_{2a}
		Z_2	Z_3
UL/DL	TP1	f_{3a}	f_{4a}
	TP2	* f_3 f_{1b} f_{2b} f_{4b}	f_{4a}
	TP3	f_{3a}	* f_4 f_{1b} f_{2b} f_{3b}
	TP4	f_{3a}	f_{4a}

		Z_4, Z_5 and Z_6	Z_1
TDD	TP1	* f_{1a}	* f_2 f_{1b}
	TP2	f_1 f_{2b} f_{3b} f_{4b}	f_{2a}
		Z_2	Z_3
UL/DL	TP1	* f_3 f_{1c}	* f_4 f_{1d}
	TP2	f_{3a}	f_{4a}

TABLE II
BANDS ASSIGNMENT FOR NEW SFR

		Z_4	Z_1	Z_5
FDD	TP1	f_{1a} f_{2a}	* f_3 f_{1b} f_{2b}	f_1 f_3 f_{2b}
	TP2	* f_1 f_2 f_{3b}	f_{3a}	f_{1a} f_{3a}
	TP3	f_1 f_2 f_{3b}	f_{3a}	* f_1 f_3 f_{2b}
		Z_2	Z_6	Z_3
UL/DL	TP1	f_{2a}	* f_2 f_3 f_{1b}	f_{1a}
	TP2	* f_2 f_{1b} f_{3b}	f_2 f_3 $1b$	f_{1a}
	TP3	f_{2a}	f_{2a} f_{3a}	* f_1 f_{2b} f_{3b}

		Z_4	Z_1	Z_5
TDD	TP1	* f_1 f_2	* f_3 f_{4a}	* f_1 f_3
	TP2	f_1 f_2 f_4	f_3	f_1 f_3 f_4
		Z_2	Z_6	Z_3
UL/DL	TP1	* f_2 f_{4b}	* f_2 f_3	* f_1 f_{4c}
	TP2	f_2	f_2 f_3 f_4	f_1

Case 3 (New SFR in FDD Systems): The proposed scheme is presented at the top part of Table II. Each f_i, $i = 1, 2, 3$ of the reference SFR is divided into two chunks f_{ia} and f_{ib} with the same $|f_{ib}|$ $\forall i$. Each frame is divided into 3 TPs of $\frac{N_{\rm sym}}{3}$ (=integer) OFDMA symbols each. The frame offsets are set as $\tau_1 = \tau_6 = 0$, $\tau_2 = \tau_4 = \frac{N_{\rm sym}}{3}$, and $\tau_3 = \tau_5 = \frac{2N_{\rm sym}}{3}$. The inner zones get additional resource amount of $|f_{ib}|$ over their first two TPs while the outer zones have additional resource amount of $2|f_{ib}|$ over their first TP.

Case 4 (New SFR in TDD Systems): The bottom part of Table II illustrates the proposed scheme. Similar to Case 2, there are no frame offsets. Different from the reference SFR, the proposed scheme divides the whole band into 4 separate chunks f_1, f_2, f_3, f_4 with the same $|f_i|$ for $i = 1, 2, 3$, and then f_4 is further trisected to f_{4a}, f_{4b}, f_{4c} with the same $|f_{4x}|$. Each frame has two TPs with $\frac{N_{\rm sym}}{2}$ (=integer) OFDMA symbols each. The outer zones get more (less) resource amount of $|f_{4x}|/2$ in their first (second) TP if compared with the reference SFR.

IV. PERFORMANCE EVALUATION AND RESULTS

A. Performance Metric and Simulation Setup

We use the post-scheduling average data rate (average of (6) over $\hat{H}_i$) which is the average spectrum efficiency that Z_i can achieve using a CSIT-exploiting scheduler with a given resource map $\mathbb{M}_i$. We adopt the Max-Fair (MF) scheduler [9] which maximizes the sum rate of a zone under the fairness condition that each selected user is assigned with only one sub-band (SB). A SB in Z_i is defined as a time-frequency resource of $N_{\rm sc}^{{\rm SB},(i)}$ contiguous subcarriers over $N_{\rm sym}^{{\rm SB},(i)}$ OFDMA symbols. Due to the frame offset τ_i, $\rho_i[n+\mu]$ in (4) and (5) is replaced by $\tilde{\rho}_i[n+\mu] \triangleq \rho_i[n+\mu-\tau_i \bmod N_{\rm sym}]$. We examine two metrics, namely, the post-scheduling average rate for outer zones $C_{\rm outer}$ and that for the whole system $C_{\rm overall}$. Based on (7), they are $C_{\rm outer}$=$\frac{\sum_{i\in\{4,5,6\}} N_i^{\rm SB} C_i}{\sum_{i\in\{4,5,6\}} N_i^{\rm SB}}$ and $C_{\rm overall}$=$\frac{\sum_{\forall i} N_i^{\rm SB} C_i}{\sum_{\forall i} N_i^{\rm SB}}$ where $N_i^{\rm SB}$ denotes the number of SBs of Z_i.

We consider a two-tier FFR multi-cell OFDMA network composed of 19 cells in DL. The system has $N_{\rm DFT} = 1024$ with 648 used subcarriers for FDD and $N_{\rm DFT} = 2048$ with 1296 used subcarriers for TDD. The carrier frequency is 2.1 GHz, the subcarrier spacing is 15 kHz, and the symbol duration is $T_s = 71.35\mu s$. Each frame has $N_{\rm sym} = 12$ OFDMA symbols. Both path loss and antenna gain models are adopted according to the Urban Macro scenario [11]. The radius of inner zones is half of the cell radius. Users are uniformly distributed in respective zones and perfect power control for path loss compensation is assumed; thus, inter-site distance does not affect the performance. We evaluate two cases of inter-site distance (1732 meters and 500 meters) [11], and find their performance results are essentially the same. For the CSIT model in (3), we use $\mu = 12$, $\sigma_{\hat{H}}^2 = 1 - \sigma_e^2$ (i.e., minimum mean square error (MMSE) estimator), and $\sigma_e^2 = 10^{-3}$ if not mentioned otherwise. $R_t(\Delta)$ in (1) is set as $e^{-(\pi f_{\rm D}\Delta)^2}$ [9] where $f_{\rm D}$ is the maximum Doppler frequency.

The SB related parameters defined by $\{N_{\rm sc}^{\rm SB}; N_{\rm sym}^{\rm SB}; N_i^{\rm SB}, i = 1, 2, 3; N_k^{\rm SB}, k = 4, 5, 6\}$ are $\{18; 6; 36; 36\}$, $\{36; 12; 18; 18\}$, and $\{18; 8; 36; 72\}$ for case 1, 2, 3, respectively, of both schemes. For case 4, they are $\{36; 12; 24; 48\}$ for the reference scheme and $\{36; 12; 20; 44\}$ for the proposed scheme. The differences in parameter values are due to different duplexing and frequency partitioning. In each zone, the number of users is the same as the number of SBs. In the following figures,"Ref." and "Pro." denote the reference scheme and the proposed scheme, while "S1" and "S2" represent the first and second effective SNRs.

B. Results and Discussions

Fig. 2 shows the post-scheduling rate versus SNR ($\triangleq \frac{P_{\rm tx}^{(i)} \zeta^{(i)}}{\sigma_{\rm N}^2}$) for the outer zones in a system with mobile speed of 120 km/h in all zones. The proposed schemes outperform their respective reference schemes by about 31%, 7%, 21% and 13% for case 1, 2, 3 and 4 in outer zones (approximately the same % at different SNRs). In terms of the overall post-scheduling rate of the system, the proposed schemes yield about 43%, −4%, 16% and −3% gains for case 1, 2, 3 and 4 over the reference schemes; the plots are omitted due to the page limit. We also investigated a scenario where the mobile speed is 60 km/h in the inner zones and 120km/h in the outer zones (results for outer zones shown in Fig. 2). The proposed schemes yield rate gains of 33%, 5%, 10%, 2% for the overall

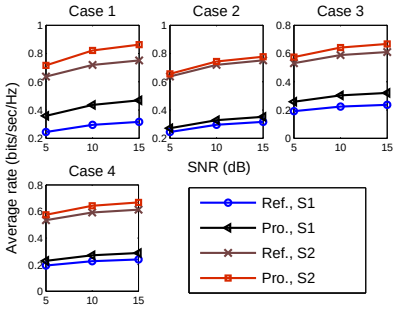

Fig. 2. Comparison of the outer zone average rate between the proposed and reference schemes

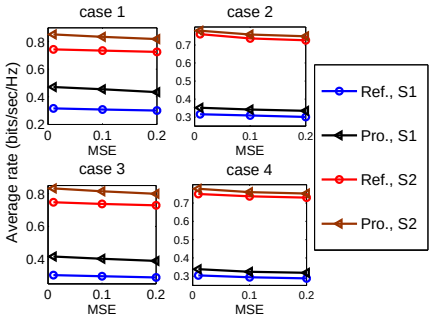

Fig. 3. Post-scheduling rates under different levels of CSIT MSE at SNR = 10 dB.

system performance of the 4 cases. The plots are omitted due to the page limit.

Next, Fig. 3 presents the impact of the CSIT mean squared error (MSE) σ_e^2 on the post-scheduling rate of the outer zones for CSIT MSE levels of 10^{-3}, 0.1, and 0.2 at the mobile speed of 120 km/h. Increased CSIT MSE causes slight rate loss but the advantages of the proposed schemes over the reference ones are still sustained.

We also investigated the performances at mobile speeds of 30 km/h, 60 km/h, and 120 km/h and SNR of 10 dB. The spectrum efficiency gains of the proposed approach for outer zones at the above speeds are respectively about 6%, 14%, 31% for case 1, 2%, 4%, 7% for case 2, 4%, 9%, 21% for case 3, and 10%, 12%, 14% for case 4. The overall spectrum efficiency gains (all zones) of the proposed approach at the above speeds are respectively about 15%, 25%, 43% for case 1, 6%, 3%, -3% for case 2, 5%, 9%, 16% for case 3, and 4%, 2%, -4% for case 4. The plots are omitted due to the page limit. Apart from TDD cases at 120 km/h which slightly sacrifice the overall performance for the benefits of outer zones, the proposed schemes yield performance improvements for outer zones as well as the overall system.

V. Conclusion

We have presented new FFR patterns for enhancing spectrum efficiency of multi-cell OFDMA systems in time-varying channels for both FDD and TDD schemes. All coverage zones of FDD and the outer zones of TDD benefit from exploiting both CSIT accuracy levels of different coverage zones and enhanced frequency domain degrees of freedom in scheduling. The inner zones of TDD may slightly sacrifice CSIT accuracy for the benefit of the outer zones while gaining enhanced frequency domain degrees of freedom in scheduling. The simulation results illustrate that the proposed FFR schemes are effective in addressing spectrum efficiency bottle-neck of outer coverage zones while enhancing or sustaining the overall system performance.

References

[1] N. Himayat and S. Talwar, "Interference management for 4G cellular standards," *IEEE Commun. Mag.,* pp. 86–92, Aug. 2010.

[2] T. D. Novlan, R. K. Ganti, A. Ghosh and J. G. Andrews, "Analytical evaluation of fractional frequency reuse for OFDMA cellular networks," *IEEE Trans. Wireless Commun.,* vol. 10, no. 12, pp. 4294–4305, Dec. 2011.

[3] Z. Xu, G. Y. Li, C. Yang and X. Zhu, "Throughput and optimal threshold for FFR schemes in OFDMA cellular networks," *IEEE Trans. Wireless Commun.,* vol. 11, no. 8, pp. 2776–2785, Aug. 2012.

[4] R. Ghaffar and R. Knopp, "Interference suppression strategy for cell-edge users in the downlink," *IEEE Trans. Wireless Commun.,* vol. 11, no. 1, pp. 154–165, Jan. 2012.

[5] A. P. Kannu and P. Schniter, "Design and analysis of MMSE pilot-aided cyclic-prefixed block transmission for doubly selective channels" *IEEE Trans. Signal Processing,* vol. 56, no. 3, pp. 1148–1160, Mar. 2008.

[6] Z. Tang, R. C. Cannizzaro, G. Leus, and P. Banelli, "Pilot-assisted time-varying channel estimation for OFDM systems," *IEEE Trans. Signal Processing,* vol. 55, no. 5, pp. 2226–2238, May 2007.

[7] W. Qiu, H. Minn, and C. C. Chong, "An efficient diversity exploitation in multiuser time-varying frequency-selective fading channels," *IEEE Trans. Commun.,* vol. 59, no. 8, pp. 2172–2184, Aug. 2011.

[8] B. Kecicioglu, H. Minn, and C.-C. Chong, "Intra-frame transmission adaptation for fast fading MIMO-OFDMA systems," *IEEE Trans. Commun.,* vol. 59, no. 9, pp. 2585–2594, Sept. 2011.

[9] P. Yen, B. Xie, and H. Minn, "Collaborative multi-system channelization," under revision in *IEEE Trans. Wireless Commun.,* www.utdallas.edu/∼Hlaing.Minn/CMSC.pdf

[10] F. Khan, *LTE for 4G Mobile Broadband: Air Interface Technologies and Performance,* First Ed. Cambridge University Press, 2009.

[11] 3GPP TR 36.814: "Evolved Universal Terrestrial Radio Access (E-UTRA): Further advancements for E-UTRA physical layer aspects," Release 9, Mar. 2010.